Published in final edited form as:

Psychiatry Res. 2015 November 30; 234(2): 164–171. doi:10.1016/j.pscychresns.2015.08.015.

Effects of acute tryptophan depletion on raphé functional connectivity in depression

Jodi J. Weinstein[a,*], **Baxter P. Rogers**[a,b,c], **Warren D. Taylor**[a,d], **Brian D. Boyd**[a], **Ronald L. Cowan**[a,b], **K. Maureen Shelton**[a], and **Ronald M. Salomon**[e,**]

[a]Department of Psychiatry, Vanderbilt University Medical Center (VUMC), Nashville, TN, USA

[b]Department of Radiology and Radiological Sciences, VUMC, Nashville, TN, USA

[c]Department of Biomedical Engineering, Vanderbilt University

[d]The Geriatric Research, Education, and Clinical Center (GRECC), VA Medical Center, Tennessee Valley Healthcare System, USA

[e]Psychiatric Research Institute, University of Arkansas for Medical Sciences, Little Rock, AR, USA

Abstract

Depression remains a great societal burden and a major treatment challenge. Most antidepressant medications target serotonergic raphé nuclei. Acute tryptophan depletion (ATD) modulates serotonin function. To better understand the raphé's role in mood networks, we studied raphé functional connectivity in depression. Fifteen depressed patients were treated with sertraline for 12 weeks and scanned during ATD and sham conditions. Based on our previous findings in a separate cohort, resting state MRI functional connectivity between raphé and other depression-related regions (ROIs) was analyzed in narrow frequency bands. ATD decreased raphé functional connectivity with the bilateral thalamus within 0.025–0.05 Hz, and also decreased raphé functional connectivity with the right pregenual anterior cingulate cortex within 0.05–0.1 Hz. Using the control broadband filtlter 0.01–0.1 Hz, no significant differences in raphé-ROI functional connectivity were observed. Post-hoc analysis by remission status suggested increased raphé functional connectivity with left pregenual anterior cingulate cortex in remitters (n = 10) and decreased raphé functional connectivity with left thalamus in non-remitters (n = 5), both within 0.025–0.05 Hz. Reducing serotonin function appears to alter coordination of these mood-related

*Correspondence to: Columbia University Medical Center, Department of Psychiatry and New York State Psychiatric Institute, 1051 Riverside Drive, New York, NY 10032, USA. **Correspondence to: University of Arkansas Medical School Psychiatric Research Institute, 4301 West Markham Street, Slot 554, Little Rock, AR 72205, USA. jodi.j.weinstein@aya.yale.edu (J.J. Weinstein).

Contributors

Dr. Weinstein contributed to analysis design, image processing and manuscript creation. Dr. Rogers contributed to analysis design, image processing and manuscript creation. Dr. Taylor contributed to analysis design and creation of this manuscript. Mr. Boyd contributed to image processing and creation of this manuscript. Dr. Cowan contributed to study design and analysis. Ms. Shelton contributed to subject recruitment, data analysis, and image processing. Dr. Salomon piloted and contributed to all phases of this research.

Conflicts of interest

None of the authors have any potential conflicts of interest.

Preliminary data was presented as poster abstracts for Society of Biological Psychiatry (2014) and American College of Neuropsychopharmacology (2014).

networks in specific, low frequency ranges. For examination of effects of reduced serotonin function on mood-related networks, specific low frequency BOLD fMRI signals can identify regions implicated in neural circuitry and may enable clinically-relevant interpretation of functional connectivity measures. The biological significance of these low frequency signals detected in the raphé merits further study.

Keywords

SSRI antidepressant; Serotonin; fMRI; Frequency; Thalamus; Anterior cingulate

1. Introduction

Depression remains a great societal burden and a major treatment challenge. Depression and suicide are associated with altered serotonin function (Maes et al., 1995; Delgado et al., 1999; Engstrom et al., 1999; Caspi et al., 2003; Bach-Mizrachi et al., 2006, 2008; Meyer, 2007). Altered serotonergic markers in depression and suicide have been identified specifically in the raphé nuclei (Bach-Mizrachi et al., 2006, 2008). Serotonin and the raphé are targets of most antidepressant medications (Scuvee-Moreau and Dresse, 1979; Blier and El Mansari, 2013).

Depression and its treatments are also associated with altered functional connectivity across multiple neural networks (Greicius et al., 2007; Fales et al., 2009; Sheline et al., 2010; Wang et al., 2012; Zhu et al., 2012; Li et al., 2013; Posner et al., 2013), but have not been linked to regions associated with specific neurotransmitter function. Changes in functional connectivity of the raphé during tryptophan depletion were recently reported (Salomon et al., 2011) and may be a promising biomarker for depression. Further exploration of this proxy measure of serotonergic activity is needed.

Functional magnetic resonance imaging (fMRI) connectivity metrics depend on specific frequencies of blood oxygen level dependent (BOLD) activation and anatomical projections between the involved regions. While the BOLD fMRI signal does not directly measure neural behavior, it has been correlated with measures of neural activity at specific frequencies (Logothetis and Wandell, 2004; Scholvinck et al., 2010; Magri et al., 2012). Frequencies of BOLD activation in the raphé may be influenced by raphé neuron activity. Spontaneous firing rates of neurons in the raphé occur within a range of 0.5–2.5 Hz (Aghajanian et al., 1978), which overlaps with frequencies detectable by fMRI. Raphé stimulation at low (0.5 Hz) frequencies produces an increase in serotonin release, differing markedly from higher frequency (10 Hz) stimulation which is associated with decreases in release (Sheard and Aghajanian, 1968). Further, models of depression are associated with changes in raphé firing rates at low (0.2 Hz) frequencies (Yavari et al., 1993). Low (0.3 Hz) frequency activity in the raphé also appears to be related to antidepressant effects (Sheard et al., 1972). Local firing rate adjustments during serotonin-reuptake inhibitor (SRI) treatments, such as sertraline, coincide with mood response (Blier et al., 1987; de Montigny et al., 1990; Chaput et al., 1991; Blier and de Montigny, 1994; Owens, 1996; Evans et al.,

2008). Together this evidence indicates that patterns of neuronal activity within the raphé relates significantly to depressive symptomatology and response to treatment.

Differential functional coupling of the raphé with extra-raphé regions likely relies on neuronal projections of the serotonin network, since the other neurons in the raphé are local interneurons. Serotonergic neurons from the brainstem pontomesencephalic raphé (which we will refer to here as dorsal raphé) project broadly to limbic cortical and other regions, including the thalamus (Baker et al., 1990, 1991a; Jacobs and Azmitia, 1992). Reciprocally, feedback from cortical regions, including the medial prefrontal cortex and subgenual anterior cingulate cortex, provides rapid and reversible effects on serotonergic neuronal function in the raphé (Amat et al., 2005; Gabbott et al., 2005; Warden et al., 2012). These anatomical and functional relationships with the raphé predict a role for raphé connectivity using fMRI connectivity approaches.

To test for changes in raphé functional connectivity with mood-related regions, a challenge paradigm is useful. Modulation of serotonin precursor availability by acute tryptophan depletion (ATD) decreases serotonin synthesis in the raphé and has been associated with worsening mood (Delgado et al., 1990). ATD alters intra-raphé activation frequencies and raphé-to-other-region functional connectivity (Salomon et al., 2011).

In the present study, MRI functional connectivity was analyzed in narrow frequency ranges comparable to those used in the prior study, but using a new, prospectively sertraline-treated, depressed cohort. Based on findings from the prior study, we hypothesized that raphé-to-ROI functional connectivity would decrease with reduced serotonin availability during ATD. As in the prior study of connectivity with the dorsal raphé, we selected brain regions (ROIs) implicated in the pathophysiology of depression or known to be rich in serotonergic innervation.

2. Methods

This study of ATD effects on raphé activation was designed with considerable caution regarding the reliability of changes in fMRI signal in a region putatively identified as anatomically consistent with dorsal raphé, with full awareness and many precautions to limit the risk that nearby tissues might be involved.

2.1. Design and sample

An institution-wide email solicited depressed adults, age 18–50, who were medication-free for at least 4 weeks. A current DSM-IV-TR diagnosis of major depressive disorder was determined by clinical interview and confirmed with a structured diagnostic interview using the Mini International Neuropsychiatric Interview, MINI (Sheehan et al., 1998). Included participants also scored 18 or higher on the 17-item Hamilton rating scale for depression (HAM-D) (Hamilton, 1960) and remission was defined as post-sertraline treatment HAM-D score less than eight.

Participants were excluded for other current primary psychiatric diagnosis, current or prior need for inpatient management, sertraline failure or documented treatment-resistance,

substance use within 1 month, daily nicotine use, pregnancy or lactation, oral contraceptive use, migraine, hepatitis, endocrinopathy, or metal implants. All participants provided signed informed consent before beginning study procedure. The Vanderbilt Institutional Review Board approved this study.

All participants were treated with sertraline 50 mg daily for 1 week, then 100 mg for 11 weeks. Participants were allowed 0.5 mg lorazepam for 3 doses in the first week of sertraline. Beyond the first week, all participants were restricted to sertraline monotherapy. Clinical visits occurred every 1–2 weeks during the treatment period. HAM-D assessments were completed at baseline and at each follow-up visit. After 12 weeks of treatment, each subject participated in two random-sequence, double-blind test days that were one week apart. Each test day morning consisted of General Clinical Research Center admission, HAM-D mood rating, blood draw for plasma tryptophan concentration, and administration of either the sham or ATD diet. Randomization and blinding was performed by the Vanderbilt Investigational Drug Service, which prepared the amino acid mixtures for both diets. Active ATD amino acid (100 g, 'full-strength') mixtures contained 15 amino acids in the balance found in human milk, but without tryptophan, as detailed previously (Delgado et al., 1990; Salomon et al., 2011). Control diets were identical, but included L-tryptophan. Six hours later (at 3 pm), HAM-D mood rating and blood sampling were repeated, immediately prior to the 45–60-min MRI scan. Morning and afternoon mood ratings used all items from the HAM-D, with carry-forward of sleep and appetite items through the day. The participant was given a normal, tryptophan-rich meal after the conclusion of the scan, regardless of which diet was received. One week later, the test day procedure was repeated with the alternate diet (*i.e.* if the participant had first received the ATD diet, the procedure was repeated with the sham diet).

2.2. MRI acquisition

Imaging data were collected on a 3T Phillips Integra scanner. For each session the scan sequence included a 3D T1 anatomical (6.5 min, 1 mm^3 isotropic voxel size) and a 6.7 min resting-state BOLD scan (200 volumes, TR 2000 msec, TE 25 msec, 30 slices, 3.75 × 3.75 mm^2 in-plane resolution, 4.5 mm thick and 0.5 mm gap). For the resting-state scans, participants were instructed to lie still and close their eyes but stay awake.

2.3. Data analysis

2.3.1. Preprocessing—Structural and functional imaging data was preprocessed using SPM8 (Friston et al., 1994) toolbox for Matlab (MathWorks, Inc., Massachusetts, United States). For intra-subject comparability between sessions, a mean structural image was calculated for each subject across conditions prior to segmentation. We applied slice-timing and motion correction to each functional session. The mean functional image was then calculated and used to create a coregistration transform for each of the sessions' functional data to the mean structural image. Finally, for each subject, the structural, subject-specific raphé ROI, and functional volumes were all normalized to ICBM-152 MNI (Montreal Neurologic Institute) template space to enable inter-subject comparability.

2.3.2. Region of interest selection and identification

2.3.2.1. Raphé: Due to its small anatomical size and nearby nonraphé structures, the subject-specific dorsal raphé was hand-drawn conservatively on the structural image, as described previously (Salomon et al., 2011). The pontomesencephalic pontine raphé region (approximating dorsal portions) was defined on the first transverse slice where both cerebral peduncles were well-defined immediately superior to the pons, one transverse anatomical slice (1 mm) superior to the isthmus and immediately anterior to the fourth ventricle. This slice was parallel and 16–30 mm inferior to the transverse plane defined by the anterior and posterior commissures. Due to the lack of clear anatomical boundaries for this region from the surrounding regions, the width of the dorsal raphé nucleus was defined as one third the total width of the midbrain at that level and a height of 3 (mm) voxels. The posterior border was defined 2 mm anterior to the aqueduct (Baker et al., 1990, 1991a, 1991b). We deliberately did not use smoothing of functional data in order to minimize contamination from nearby tissues. Due to the potential for displacement of this small region during normalization, we reviewed the raphé ROI's location on each subject's structural image after normalization and adjusted its location to ensure that it was still correctly placed on the dorsal raphé (Fig. 1).

2.3.2.2. Target regions: The anterior thalamus and pregenual anterior cingulate cortex (pgACC) regions replicated those in our prior study using MNI coordinates from WFU Pick Atlas (Tzourio-Mazoyer et al., 2002; Maldjian et al., 2003, 2004). Additional exploratory ROIs with rich serotonergic innervation and known changes in depression included the subgenual anterior cingulate cortex (sgACC) and ventromedial prefrontal cortex (vmPFC). Further, cognitive exploratory targets included dorsolateral prefrontal cortex (dlPFC), and posterior cingulate cortex (PCC). The sgACC coordinates were based on Mayberg et al. (1997). The remaining three regions used CONN toolbox standards (see Table 1).

2.3.3. Functional connectivity analysis—An ROI-to-ROI bivariate correlation analysis was facilitated by CONN Functional Connectivity toolbox for Matlab, version13o (Whitfield-Gabrieli and Ford, 2012; Whitfield-Gabrieli and Nieto-Castanon, 2012). Regression removed effects of motion (6 rigid body parameters and their first differences) and 5 principal components from each of the white matter and cerebrospinal fluid ROIs.

Bandpass temporal frequency filtering isolated narrow frequency bands to closely mimic the prior study, which had used a wavelet procedure that influenced frequency boundaries, giving non-discrete cut-offs with odd values of 0.25–0.125, 0.125–0.0625, 0.0625–0.03125 Hz, and a residual band of <0.03125 Hz. In CONN, finite impulse response (FIR) filtering provides discrete frequency cut-offs so that boundaries could be selected for separate analyses at 0.01–0.025 Hz, 0.025–0.05 Hz, and 0.05–0.1 Hz. An analysis using a standard fMRI frequency filtlter of 0.01–0.1 Hz was also conducted for comparison.

In second-level analyses, we computed the difference in functional connectivity between sham and ATD conditions for each raphé-to-ROI pair. We used a general linear model with separate categorical predictors for remitters and non-remitters, where remission was defined as post-sertraline treatment HAM-D score less than eight. When we contrasted diet

conditions across all subjects, predictors for remitters and non-remitters were combined with weights proportionate to their respective subgroup size.

3. Results

3.1. Demographics

Phone screens yielded 37 individuals eligible for interview, of whom 18 entered and 17 completed the protocol. Data were dropped for non-adherence to the protocol (n = 1) and for an inconsistent blind per pharmacy and laboratory documentation (n = 1), giving a final sample of 15. Mean age was 35 years (SD = 7, range 25–46). Nine (60%) were male. Mean HAM-D score before SSRI was 21 and scores did not significantly differ between subsequent remitters (mean = 20, SD = 1.9) and non-remitters (mean = 23, SD = 5.6, t = 1.6, 13 df, p = 0.13). Sertraline 100 mg daily was tolerated in all subjects. Remission (HAM-D < 8) was achieved in 10 of the 15 subjects (7 males and 3 females). Mean HAM-D scores after treatment (*i.e.* at week-12 clinic visit) were 3.8 (SD = 2.6) in remitters and 15.8 (SD = 5.6) in non-remitters (t = 5.3, df = 13, p = 0.0002). Participants' morning pre-diet HAM-D scores did not significantly differ between sham and ATD test days (mean pre-sham = 6.7, SD = 4.1, mean pre-ATD = 7.9, SD = 5.4, t = 1.07, df = 14, p = 0.305).

3.2. Tryptophan depletion

Post-ATD plasma tryptophan levels in all participants dropped below 15 μmol/L (mean = 3.8), compared to a range of 20–136 μmol/L (mean = 56.4) for sham diets (mean difference = 53.4, t = 6.63, df = 13, p < 0.0001). No individual showed a mood relapse with ATD (HAM-D score pre-ATD mean = 7.9, SD = 5.4, post-ATD mean = 7.2, SD = 4.6, t = 1.16, df = 14, p = 0.265), and mean mood scores did not change significantly compared to morning baseline (t = 0.90, df = 14, p = 0.38). There were no serious adverse events and the study protocol was well-tolerated.

3.3. Functional connectivity analysis

Analysis of motion on a per voxel basis revealed that the 95th percentile of displacement relative to the preceding volume was 0.8 mm or less in all sessions from all subjects, so none were rejected for excessive movement.

Table 2 shows functional connectivity results for the raphé with the selected ROIs after SSRI treatment. In all cases, differences in functional connectivity are reported as sham minus ATD conditions. When we examined all participants' data using the narrow frequency band 0.025–0.05 Hz, we found that ATD significantly altered raphé functional connectivity with both the right and left thalamus. Within 0.05–0.1 Hz, ATD decreased raphé functional connectivity with the right pregenual ACC. Using the control broadband filtlter 0.01–0.1 Hz, no significant differences in raphé-ROI functional connectivity were observed with ATD.

In exploratory analyses of functional connectivity considering remitted and non-remitted subjects separately, raphé functional connectivity changes with ATD were identified only in the frequency range 0.025–0.05 Hz. In remitters (n = 10), ATD *increased* functional connectivity in this frequency range between the raphé and left pregenual ACC. In the non-

remitters (n = 5), ATD *decreased* functional connectivity between the raphé and left thalamus. Additionally, when stratified by remission status, HAM-D score in non-remitters significantly correlated with raphé functional connectivity with the right anterior thalamus in 0.025–0.05 Hz (r = −0.96, p < 0.01) and left pregenual ACC in 0.025–0.05 Hz (r = 0.89, p = 0.04). In remitters, higher HAM-D score trended to correlate with raphé functional connectivity with the left anterior thalamus in 0.01–0.025 Hz (r = −0.62, p < 0.06).

4. Discussion

This study shows ATD effects in remitted depression on a region consistent with the pontomesencephalic dorsal raphé using resting-state functional connectivity. Following the hypothesis that was based on findings from our previous study (Salomon et al., 2011), we again found that ATD effects on raphé functional connectivity were limited to a narrow low frequency bandwidth. Again, as in the first study, we did not observe effects of ATD on raphé functional connectivity in the full bandwidth in all subjects. This is consistent with our previous findings in SSRI-treated patients following challenges with ATD or sham diets (Salomon et al., 2011).

In this new data set, significant decreases in functional connectivity for the raphé with both the left and right thalamus were again specific to the frequency range 0.025–0.05 Hz (see note below regarding filtering methods). Additionally, significant decreases in functional connectivity between raphé and pregenual ACC were specific to the 0.05–0.1 Hz frequency range. Since these effects were not detected using the customary frequency range of 0.01–0.1 Hz, narrower frequency bands appear to be critical for detecting changes in raphé functional connectivity. Imaging measures of raphé function in depression that specify narrower frequency ranges may allow a novel probe of serotonergic neuromodulation relevant to depression.

To our knowledge, this is the first report of the effects of ATD on raphé functional connectivity in prospectively-treated depression. The prior study recruited only remitted patients, whereas the present study cohort was recruited prior to treatment initiation, allowing a secondary analysis of remitters and non-remitters. While the prior analysis used custom programming with wavelet filtlters (which have sloped frequency cut-offs), another advantage of the current study is the demonstration of raphé functional connectivity changes using more discrete frequency band cut-offs and widely-accepted image analysis tools (SPM8 and CONN). These tools utilize the functional connectivity literature-standard frequency filtering methods and also provide MNI-normalized region selection. When comparing findings from these two studies, it should be noted that the relative widths of the frequency bands were retained approximately from the previous study; the only significant difference was the starting point for decimation (or the upper bound): 0.1 Hz instead of 0.25 Hz, to be more conservative about exclusion of physiologic noise, in accordance with convention. As a result, the ranges used for the narrower frequency bandpass filtlters are not exactly identical, but are sufficiently similar to allow meaningful comparisons.

The frequency-specific property of the observed ATD-induced functional connectivity changes is not unusual. Frequency-specific properties of resting state BOLD signal have

been shown to be spatially distributed and linked to network connectivity, and examination of BOLD oscillation properties of the default mode network has revealed a distinct frequency-dependent regional composition across subjects (Baria et al., 2011), but the biological significance of these frequency ranges is unknown. There are several possible physiologic explanations for the observed ATD-induced functional connectivity changes. The anterior thalamus is rich in serotonin receptors and transporter-rich terminals (Chapin and Andrade, 2001; Marek et al., 2001; Varnas et al., 2004). Raphé serotonin neuron projections to thalamus are known to modulate thalamocortical activity (Andersen et al., 1983; McCormick, 1992; Steriade, 1999). One possibility is that the observed functional connectivity relationships represent slow oscillators and that ATD-induced functional connectivity changes are a proxy for serotonergic effects on physiologically-important slow oscillations. This variability may be related to feedback mechanisms within the serotonin system. For example, our findings for raphé-thalamic functional connectivity at frequencies < 1 Hz is analogous to the < 1 Hz thalamic oscillations observed during sleep and may inform the relationship between sleep disturbances and depression (Buysse et al., 1990).

It is also possible that diminished serotonergic transmission in depressive states may impair self-regulation of raphé firing variability. Altered serotonin function clearly plays a role in depression and its treatment (Blier and El Mansari, 2013) and a potential role for slow oscillations in serotonin function has been hypothesized (Salomon and Cowan, 2013). Changes in network activity may be modulated by raphé activity at low frequency. Such slow fluctuations <1 Hz may be generated by cell metabolic cycles, or local positive and negative tissue feedback loops (Hu et al., 2007, 2008; Novak et al., 2007; Pigolotti et al., 2007; Tiana et al., 2007; Novak and Tyson, 2008; Tsai et al., 2008). Consistent with this, changes in BOLD signal are thought to be closely related to functions of local interneurons (Gsell et al., 2006). Locally, serotonin inhibits excitatory interneurons (Adell et al., 2001; Celada et al., 2001; Martin-Ruiz et al., 2001; Ciranna, 2006; Grasso et al., 2006). ATD may weaken this inhibition, allowing an increase GABA to further inhibit serotonin release, but this too warrants further study.

While there is extensive evidence of serotonergic effects on metabolic activity (assumed to be driven primarily by neuronal activity) as measured by FDG-PET (Morris et al., 1999) and neuronal oscillations as measured by EEG and LFP recordings (comprehensively reviewed by Celada et al., 2013), it is also possible that not all changes in hemodynamics related to ATD are secondary to changes in neuronal activity. Since our fMRI measures are derived from hemodynamic properties (BOLD) and serotonin can modulate vascular flow (Kelley et al., 1988), the observed functional connectivity changes may reflect direct effects of ATD on the vasculature and/or changes in neurovascular coupling, rather than the inter-regional coordination of underlying neural activity (Chugani et al., 1999; Adnot et al., 2013; Hillman, 2014). While it is unknown whether ATD could also affect neurovascular coupling, there is little evidence to support this possibility without it also affecting neuronal activity or oscillations (Anderer et al., 2000; Tfelt-Hansen and Koehler, 2011). Moreover, since several this study's ROIs have rich serotonergic innervation and ATD-induced raphé connectivity changes were only observed with the thalamus and anterior cingulate; it is unlikely that ATD effects on neurovascular coupling would be regionally-specific among the projection sites we examined. A conservative interpretation is that our findings indicate that ATD

induced some combination changes in neural signaling, neurometabolic activity, and neurovascular coupling in specific pairs of regions within specific frequency regions. Further research is needed to clarify the underlying mechanisms of ATD-induced alterations in raphé functional coupling.

Our exploratory analyses stratified for remission suggest group-specific differences in the effect of reducing serotonin function on raphé functional connectivity. In analyses of the entire cohort, we observed a *decrease* in functional connectivity in 0.05–0.1 Hz frequency range with ATD between the raphé and the right pgACC. However, analyses of remitters alone showed an *increase* in functional connectivity at 0.025–0.05 Hz frequency range between the raphé and the left pgACC. Identification of ATD-induced changes functional connectivity with the pgACC is consistent with many findings associating the pgACC with mood changes in depression (Mayberg et al., 1997; Price and Drevets, 2010). Our preliminary findings relating raphé-pgACC functional connectivity to remission status suggest that these oscillators may fluctuate with depression severity or SSRI treatment response. As such, it is possible that raphé-pgACC connectivity may represent a biomarker of SSRI-induced remission. However, this exploratory analysis is limited by the small subgroup sample size.

Several limitations of this study must be noted. Power in this study was limited in more than one aspect. The study had a small sample size, especially for the non-remitted cohort subgroup analyses, as noted above. Decomposing our signal into narrower frequency bands also limited our power. This study was designed to test one specific hypothesis (decreased functional connectivity in thalamus-raphé at a specific frequency) and despite the small sample size and narrow frequency bands, our results support our hypothesis. If we correct for the comparison of three frequency bands, some results remain statistically significant. Raphé connectivity with the left thalamus remains highly significant (Bonferroni- corrected-p=0.02) while the right thalamus-raphé loses statistical validity (Bonferroni-corrected-p=1.5). To examine narrow frequency bands with more power in future studies, longer scans may be of greater interest.

The small size and location of the pontomesencephalic raphé raises concern for anatomical variation and partial volume effects. To minimize this concern, raphé ROIs were conservatively hand-drawn, reviewed after normalization and, also, a single placement was applied to both scans from each subject. However, deviations due to partial volume effects in the case of less serotonergic pararaphé regions would be expected to weaken the signal we are detecting, and are unlikely to produce a false-positive result. Also, if our raphé region selection overlapped with the median raphé, our finding would remain important.

Design limitations are also inherent in the target ROI selection and identification process. By using an *a priori* hypothesis that focused on a few specific ROIs, we strengthened the statistical power of our finding and minimized the risk of false positives from multiple comparisons; but we also sacrificed possible detection of any other potentially-involved regions that were not examined under our hypothesis. Since serotonergic neurons project throughout the brain, there could be many additional networks of relevance to be examined. Additionally, we identified our ROIs structurally based on established, standard coordinates;

subject-specific functionally-identified ROIs may have enabled individual specificity, but also would have limited generalizability of our results.

Although this study does not examine neural networks directly, it supports past work demonstrating that ATD is a useful probe for modulating neural networks dependent on serotonergic innervation (Kahkonen et al., 2005; Evers et al., 2006; Merens et al., 2008; Roiser et al., 2009; Daly et al., 2010; Van der Veen et al., 2010; Booij and Van der Does, 2011; Kunisato et al., 2011). This study also extends this by indirectly demonstrating involvement of pontomesencephalic raphé. ATD effects on resting state fMRI of raphé functional connectivity may yield improved techniques for understanding raphé functional changes in depression. Although the BOLD fMRI signal is not a direct measure of neural activity, this modality provides a window to examine slow frequency functional characteristics of raphé regions in humans. The fMRI measure originates from the hemodynamic response, and not directly from neural activity. When fMRI measurements are taken simultaneous with neuronal recordings, the fMRI signal does track neural oscillations (often slow oscillations) (Logothetis and Wandell, 2004; Magri et al., 2012). Our study also shows that oscillatory activity within the fMRI record relates to serotonergic state. Perhaps this supports using fMRI as an alternative to understand how oscillatory activity relates to depression, but the direct relationship between the oscillatory pattern within the fMRI signal and actual neuronal activity has yet to be established. Elucidating the relationships among actual neural activity and various measures remains a work in progress. Future investigations of slow neural oscillations and neurovascular coupling characteristics in depression may help to explain pathogenesis of depressive symptomatology and its treatment. Studies of antidepressant effects on BOLD fMRI and functional connectivity are also needed. Relationships among oscillations in different frequency ranges may have important clinical implications, such as sleep and depression, or be predictive of treatment response. Future studies of depression should examine the clinical implications of alterations in and oscillations of raphé functional connectivity.

Acknowledgments

In addition to our funding sources, the authors thank the study participants, without whom this work would not be possible. The assistance of Jennifer Blackford, Margaret Benningfield, Haleh Karbasforoushan, Jared Meggs, Sarah Jane Camper, and Xiaoyan Xu is appreciated. The study was partially supported by Grants from NIMH K23 MH01828 and R21 MH087803 (to RMS); NIDA R01 DA01537, R21 DA020149, and NIMH R21 MH073800 (to RLC); Vanderbilt CTSA grant UL1 RR024975 from NCRR/NIH (to Vanderbilt Clinical Research Center); and NIMH T32 MH018870 (JJW). The funding sources had no involvement in the conduct of this research or preparation of this article.

References

Maes M, Meltzer HY, D'Hondt P, Cosyns P, Blockx P. Effects of serotonin precursors on the negative feedback effects of glucocorticoids on hypothalamic-pituitary-adrenal axis function in depression. Psychoneuroendocrinology. 1995; 20:149–167. [PubMed: 7899535]

Delgado PL, Miller HL, Salomon RM, Licinio J, Krystal JH, Moreno FA, Heninger GR, Charney DS. Tryptophan-depletion challenge in depressed patients treated with desipramine or fluoxetine: implications for the role of serotonin in the mechanism of antidepressant action. Biol. Psychiatry. 1999; 46:212–220. [PubMed: 10418696]

Engstrom G, Alling C, Blennow K, Regnell G, Traskman-Bendz L. Reduced cerebrospinal HVA concentrations and HVA/5-HIAA ratios in suicide attempters. Monoamine metabolites in 120

suicide attempters and 47 controls. Eur. Neuropsychopharmacol.: J. Eur. Coll. Neuropsychopharmacol. 1999; 9:399–405.

Caspi A, Sugden K, Moffitt TE, Taylor A, Craig IW, Harrington H, McClay J, Mill J, Martin J, Braithwaite A, Poulton R. Influence of life stress on depression: moderation by a polymorphism in the 5-HTT gene. Science. 2003; 301:386–389. [PubMed: 12869766]

Bach-Mizrachi H, Underwood MD, Kassir SA, Bakalian MJ, Sibille E, Tamir H, Mann JJ, Arango V. Neuronal tryptophan hydroxylase mRNA expression in the human dorsal and median raphe nuclei: major depression and suicide. Neuropsychopharmacol.: Off. Publ. Am. Coll. Neuropsychopharmacol. 2006; 31:814–824.

Meyer JH. Imaging the serotonin transporter during major depressive disorder and antidepressant treatment. J. Psychiatry Neurosci. 2007; 32:86–102. [PubMed: 17353938]

Bach-Mizrachi H, Underwood MD, Tin A, Ellis SP, Mann JJ, Arango V. Elevated expression of tryptophan hydroxylase-2 mRNA at the neuronal level in the dorsal and median raphe nuclei of depressed suicides. Mol. Psychiatry. 2008; 13(507–513):465.

Scuvee-Moreau JJ, Dresse AE. Effect of various antidepressant drugs on the spontaneous firing rate of locus coeruleus and dorsal raphe neurons of the rat. Eur. J. Pharmacol. 1979; 57:219–225. [PubMed: 488160]

Blier P, El Mansari M. Serotonin and beyond: therapeutics for major depression. Philos. Trans. R. Soc. Lond. Ser. B Biol. Sci. 2013; 368:20120536. [PubMed: 23440470]

Greicius MD, Flores BH, Menon V, Glover GH, Solvason HB, Kenna H, Reiss AL, Schatzberg AF. Resting-state functional connectivity in major depression: abnormally increased contributions from subgenual cingulate cortex and thalamus. Biol. Psychiatry. 2007; 62:429–437. [PubMed: 17210143]

Fales CL, Barch DM, Rundle MM, Mintun MA, Mathews J, Snyder AZ, Sheline YI. Antidepressant treatment normalizes hypoactivity in dorsolateral prefrontal cortex during emotional interference processing in major depression. J. Affect. Disord. 2009; 112:206–211. [PubMed: 18559283]

Sheline YI, Price JL, Yan Z, Mintun MA. Resting-state functional MRI indepression unmasks increased connectivity between networks via the dorsal nexus. Proc. Natl. Acad. Sci. USA. 2010; 107:11020–11025. [PubMed: 20534464]

Wang L, Hermens DF, Hickie IB, Lagopoulos J. A systematic review of resting-state functional-MRI studies in major depression. J. Affect. Disord. 2012; 142:6–12. [PubMed: 22858266]

Zhu X, Wang X, Xiao J, Liao J, Zhong M, Wang W, Yao S. Evidence of a dissociation pattern in resting-state default mode network connectivity in first-episode, treatment-naive major depression patients. Biol. Psychiatry. 2012; 71:611–617. [PubMed: 22177602]

Li B, Liu L, Friston KJ, Shen H, Wang L, Zeng LL, Hu D. A treatment-resistant default mode subnetwork in major depression. Biol. Psychiatry. 2013; 74:48–54. [PubMed: 23273724]

Posner J, Hellerstein DJ, Gat I, Mechling A, Klahr K, Wang Z, McGrath PJ, Stewart JW, Peterson BS. Antidepressants normalize the default mode network in patients with dysthymia. JAMA Psychiatry. 2013; 70:373–382. [PubMed: 23389382]

Salomon RM, Cowan RL, Rogers BP, Dietrich MS, Bauernfeind AL, Kessler RM, Gore JC. Time series fMRI measures detect changes in pontine raphe following acute tryptophan depletion. Psychiatry Res. 2011; 191:112–121. [PubMed: 21236648]

Logothetis NK, Wandell BA. Interpreting the BOLD signal. Annu. Rev. Physiol. 2004; 66:735–769. [PubMed: 14977420]

Scholvinck ML, Maier A, Ye FQ, Duyn JH, Leopold DA. Neural basis of global resting-state fMRI activity. Proc. Natl. Acad. Sci. USA. 2010; 107:10238–10243. [PubMed: 20439733]

Magri C, Schridde U, Murayama Y, Panzeri S, Logothetis NK. The amplitude and timing of the BOLD signal reflects the relationship between local field potential power at different frequencies. J. Neurosci. Off. J. Soc. Neurosci. 2012; 32:1395–1407.

Aghajanian GK, Wang RY, Baraban J. Serotonergic and non-serotonergic neurons of the dorsal raphe: reciprocal changes in firing induced by peripheral nerve stimulation. Brain Res. 1978; 153:169–175. [PubMed: 679043]

Sheard MH, Aghajanian GK. Stimulation of the midbrain raphe: effect on serotonin metabolism. J. Pharmacol. Exp. Ther. 1968; 163:425–430. [PubMed: 4878661]

Yavari P, Vogel GW, Neill DB. Decreased raphe unit activity in a rat model of endogenous depression. Brain Res. 1993; 611:31–36. [PubMed: 8390911]

Sheard MH, Zolovick A, Aghajanian GK. Rophe neurons: effect of tricyclic antidepressant drugs. Brain Res. 1972; 43:690–694. [PubMed: 5053300]

Blier P, de Montigny C, Chaput Y. Modifications of the serotonin system by antidepressant treatments: implications for the therapeutic response in major depression. J. Clin. Psychopharmacol. 1987; 7:24S–35S. [PubMed: 3323264]

de Montigny C, Chaput Y, Blier P. Modification of serotonergic neuron properties by long-term treatment with serotonin reuptake blockers. J. Clin. Psychiatry. 1990; 51(Suppl B):4–8. [PubMed: 2175309]

Chaput Y, de Montigny C, Blier P. Presynaptic and postsynaptic modifications of the serotonin system by long-term administration of antidepressant treatments. An in vivo electrophysiologic study in the rat. Neuropsychopharmacol.: Off. Publ. Am. Coll. Neuropsychopharmacol. 1991; 5:219–229.

Blier P, de Montigny C. Current advances and trends in the treatment of depression. Trends Pharmacol. Sci. 1994; 15:220–226. [PubMed: 7940983]

Owens MJ. Molecular and cellular mechanisms of antidepressant drugs. Depression Anxiety. 1996; 4:153–159. [PubMed: 9166647]

Evans AK, Reinders N, Ashford KA, Christie IN, Wakerley JB, Lowry CA. Evidence for serotonin synthesis-dependent regulation of *in vitro* neuronal firing rates in the midbrain raphe complex. Eur. J. Pharmacol. 2008; 590:136–149. [PubMed: 18577382]

Baker KG, Halliday GM, Tork I. Cytoarchitecture of the human dorsal raphe nucleus. J. Comp. Neurol. 1990; 301:147–161. [PubMed: 2262589]

Baker KG, Halliday GM, Halasz P, Hornung JP, Geffen LB, Cotton RG, Tork I. Cytoarchitecture of serotonin-synthesizing neurons in the pontine tegmentum of the human brain. Synapse. 1991a; 7:301–320. [PubMed: 2042112]

Jacobs BL, Azmitia EC. Structure and function of the brain serotonin system. Physiol. Rev. 1992; 72:165–229. [PubMed: 1731370]

Amat J, Baratta MV, Paul E, Bland ST, Watkins LR, Maier SF. Medial prefrontal cortex determines how stressor controllability affects behavior and dorsal raphe nucleus. Nat. Neurosci. 2005; 8:365–371. [PubMed: 15696163]

Gabbott PL, Warner TA, Jays PR, Salway P, Busby SJ. Prefrontal cortex in the rat: projections to subcortical autonomic, motor, and limbic centers. J. Comp. Neurol. 2005; 492:145–177. [PubMed: 16196030]

Warden MR, Selimbeyoglu A, Mirzabekov JJ, Lo M, Thompson KR, Kim SY, Adhikari A, Tye KM, Frank LM, Deisseroth K. A prefrontal cortex-brainstem neuronal projection that controls response to behavioural challenge. Nature. 2012; 492:428–432. [PubMed: 23160494]

Delgado PL, Charney DS, Price LH, Aghajanian GK, Landis H, Heninger GR. Serotonin function and the mechanism of antidepressant action. Reversal of antidepressant-induced remission by rapid depletion of plasma tryptophan. Arch. Gen. Psychiatry. 1990; 47:411–418. [PubMed: 2184795]

Sheehan DV, Lecrubier Y, Sheehan KH, Amorim P, Janavs J, Weiller E, Hergueta T, Baker R, Dunbar GC. The Mini-International Neuropsychiatric Interview (M.I.N.I.): the development and validation of a structured diagnostic psychiatric interview for DSM-IV and ICD-10. J. Clin. Psychiatry. 1998; 59(Suppl 20):22–33. quiz 34–57. [PubMed: 9881538]

Hamilton M. A rating scale for depression. J. Neurol. Neurosurg. Psychiatry. 1960; 23:56–62. [PubMed: 14399272]

Friston KJ, Holmes AP, Worsley KJ, Poline JP, Frith CD, Frackowiak RSJ. Statistical parametric maps in functional imaging: A general linear approach. Hum. Brain Mapp. 1994; 2:189–210.

Baker KG, Halliday GM, Hornung JP, Geffen LB, Cotton RG, Tork I. Distribution, morphology and number of monoamine-synthesizing and substance P-containing neurons in the human dorsal raphe nucleus. Neuroscience. 1991b; 42:757–775. [PubMed: 1720227]

Tzourio-Mazoyer N, Landeau B, Papathanassiou D, Crivello F, Etard O, Delcroix N, Mazoyer B, Joliot M. Automated anatomical labeling of activations in SPM using a macroscopic anatomical parcellation of the MNI MRI single-subject brain. NeuroImage. 2002; 15:273–289. [PubMed: 11771995]

Maldjian JA, Laurienti PJ, Kraft RA, Burdette JH. An automated method for neuroanatomic and cytoarchitectonic atlas-based interrogation of fMRI data sets. NeuroImage. 2003; 19:1233–1239. [PubMed: 12880848]

Maldjian JA, Laurienti PJ, Burdette JH. Precentral gyrus discrepancy in electronic versions of the Talairach atlas. NeuroImage. 2004; 21:450–455. [PubMed: 14741682]

Whitfield-Gabrieli S, Ford JM. Default mode network activity and connectivity in psychopathology. Annu. Rev. Clin. Psychol. 2012; 8:49–76. [PubMed: 22224834]

Whitfield-Gabrieli S, Nieto-Castanon A. Conn: a functional connectivity toolbox for correlated and anticorrelated brain networks. Brain Connect. 2012; 2:125–141. [PubMed: 22642651]

Baria AT, Baliki MN, Parrish T, Apkarian AV. Anatomical and functional assemblies of brain BOLD oscillations. J. Neurosci. Off. J. Soc. Neurosci. 2011; 31:7910–7919.

Chapin EM, Andrade R. A 5-HT(7) receptor-mediated depolarization in the anterodorsal thalamus. I. Pharmacological characterization. J. Pharmacol. Exp. Ther. 2001; 297:395–402. [PubMed: 11259568]

Marek GJ, Wright RA, Gewirtz JC, Schoepp DD. A major role for thalamocortical afferents in serotonergic hallucinogen receptor function in the rat neocortex. Neuroscience. 2001; 105:379–392. [PubMed: 11672605]

Varnas K, Halldin C, Hall H. Autoradiographic distribution of serotonin transporters and receptor subtypes in human brain. Hum. Brain Mapp. 2004; 22:246–260. [PubMed: 15195291]

Andersen E, Rigor B, Dafny N. Electrophysiological evidence of concurrent dorsal raphe input to caudate, septum, habenula, thalamus hippocampus, cerebellum and olfactory bulb. Int. J. Neurosci. 1983; 18:107–115. [PubMed: 6302024]

McCormick DA. Neurotransmitter actions in the thalamus and cerebral cortex and their role in neuromodulation of thalamocortical activity. Prog. Neurobiol. 1992; 39:337–388. [PubMed: 1354387]

Steriade M. Brainstem activation of thalamocortical systems. Brain Res. Bull. 1999; 50:391–392. [PubMed: 10643450]

Buysse DJ, Jarrett DB, Miewald JM, Kupfer DJ, Greenhouse JB. Minute-by-minute analysis of REM sleep timing in major depression. Biol. Psychiatry. 1990; 28:911–925. [PubMed: 2268693]

Salomon RM, Cowan RL. Oscillatory serotonin function in depression. Synapse. 2013; 67:801–820. [PubMed: 23592367]

Hu K, Scheer FA, Ivanov P, Buijs RM, Shea SA. The suprachiasmatic nucleus functions beyond circadian rhythm generation. Neuroscience. 2007; 149:508–517. [PubMed: 17920204]

Novak B, Tyson JJ, Gyorffy B, Csikasz-Nagy A. Irreversible cell-cycle transitions are due to systems-level feedback. Nat. Cell Biol. 2007; 9:724–728. [PubMed: 17603504]

Pigolotti S, Krishna S, Jensen MH. Oscillation patterns in negative feedback loops. Proc. Nat. l Acad. Sci. USA. 2007; 104:6533–6537.

Tiana G, Krishna S, Pigolotti S, Jensen MH, Sneppen K. Oscillations and temporal signalling in cells. Phys. Biol. 2007; 4:R1–R17. [PubMed: 17664651]

Hu K, Scheer FA, Buijs RM, Shea SA. The endogenous circadian pacemaker imparts a scale-invariant pattern of heart rate fluctuations across time scales spanning minutes to 24 h. J. Biol. Rhythm. 2008; 23:265–273.

Novak B, Tyson JJ. Design principles of biochemical oscillators. Nat. Rev. Mol. Cell Biol. 2008; 9:981–991. [PubMed: 18971947]

Tsai TY, Choi YS, Ma W, Pomerening JR, Tang C, Ferrell JE Jr. Robust, tunable biological oscillations from interlinked positive and negative feedback loops. Science. 2008; 321:126–129. [PubMed: 18599789]

Gsell W, Burke M, Wiedermann D, Bonvento G, Silva AC, Dauphin F, Buhrle C, Hoehn M, Schwindt W. Differential effects of NMDA and AMPA glutamate receptors on functional magnetic resonance imaging signals and evoked neuronal activity during forepaw stimulation of the rat. J. Neurosci. Off. J. Soc. Neurosci. 2006; 26:8409–8416.

Adell A, Celada P, Artigas F. The role of 5-HT1B receptors in the regulation of serotonin cell firing and release in the rat brain. J. Neurochem. 2001; 79:172–182. [PubMed: 11595769]

Celada P, Puig MV, Casanovas JM, Guillazo G, Artigas F. Control of dorsal raphe serotonergic neurons by the medial prefrontal cortex: Involvement of serotonin-1A, GABA(A), and glutamate receptors. J. Neurosci.: Off. J. Soc. Neurosci. 2001; 21:9917–9929.

Martin-Ruiz R, Puig MV, Celada P, Shapiro DA, Roth BL, Mengod G, Artigas F. Control of serotonergic function in medial prefrontal cortex by serotonin-2A receptors through a glutamate-dependent mechanism. J. Neurosci.: Off. J. Soc. Neurosci. 2001; 21:9856–9866.

Ciranna L. Serotonin as a modulator of glutamate- and GABA-mediated neurotransmission: implications in physiological functions and in pathology. Curr. Neuropharmacol. 2006; 4:101–114. [PubMed: 18615128]

Grasso C, Li Volsi G, Licata F, Ciranna L, Santangelo F. Aminergic control of neuronal firing rate in thalamic motor nuclei of the rat. Arch. Ital. Biol. 2006; 144:173–196. [PubMed: 16977832]

Morris JS, Smith KA, Cowen PJ, Friston KJ, Dolan RJ. Covariation of activity in habenula and dorsal raphe nuclei following tryptophan depletion. NeuroImage. 1999; 10:163–172. [PubMed: 10417248]

Celada P, Puig MV, Artigas F. Serotonin modulation of cortical neurons and networks. Front. Integr. Neurosci. 2013; 7:25. [PubMed: 23626526]

Kelley C, D'Amore P, Hechtman HB, Shepro D. Vasoactive hormones and cAMP affect pericyte contraction and stress fibres in vitro. J. Muscle Res. Cell Motil. 1988; 9:184–194. [PubMed: 2458383]

Chugani DC, Niimura K, Chaturvedi S, Muzik O, Fakhouri M, Lee ML, Chugani HT. Increased brain serotonin synthesis in migraine. Neurology. 1999; 53:1473–1479. [PubMed: 10534254]

Adnot S, Houssaini A, Abid S, Marcos E, Amsellem V. Serotonin transporter and serotonin receptors. Handb. Exp. Pharmacol. 2013; 218:365–380. [PubMed: 24092348]

Hillman EM. Coupling mechanism and significance of the BOLD signal: a status report. Annu. Rev. Neurosci. 2014; 37:161–181. [PubMed: 25032494]

Anderer P, Saletu B, Pascual-Marqui RD. Effect of the 5-HT(1A) partial agonist buspirone on regional brain electrical activity in man: a functional neuroimaging study using low-resolution electromagnetic tomography (LOR-ETA). Psychiatry Res. 2000; 100:81–96. [PubMed: 11114494]

Tfelt-Hansen PC, Koehler PJ. One hundred years of migraine research: major clinical and scientific observations from 1910 to 2010. Headache. 2011; 51:752–778. [PubMed: 21521208]

Mayberg HS, Brannan SK, Mahurin RK, Jerabek PA, Brickman JS, Tekell JL, Silva JA, McGinnis S, Glass TG, Martin CC, Fox PT. Cingulate function in depression: a potential predictor of treatment response. Neuroreport. 1997; 8:1057–1061. [PubMed: 9141092]

Price JL, Drevets WC. Neurocircuitry of mood disorders. Neuropsychopharmacol.: Off. Publ. Am. Coll. Neuropsychopharmacol. 2010; 35:192–216.

Kahkonen S, Makinen V, Jaaskelainen IP, Pennanen S, Liesivuori J, Ahveninen J. Serotonergic modulation of mismatch negativity. Psychiatry Res. 2005; 138:61–74. [PubMed: 15708302]

Evers EA, van der Veen FM, van Deursen JA, Schmitt JA, Deutz NE, Jolles J. The effect of acute tryptophan depletion on the BOLD response during performance monitoring and response inhibition in healthy male volunteers. Psychopharmacology. 2006; 187:200–208. [PubMed: 16710715]

Merens W, Booij L, Haffmans PJ, van der Does A. The effects of experimentally lowered serotonin function on emotional information processing and memory in remitted depressed patients. J. Psychopharmacol. 2008; 22:653–662. [PubMed: 18308809]

Roiser JP, Levy J, Fromm SJ, Nugent AC, Talagala SL, Hasler G, Henn FA, Sahakian BJ, Drevets WC. The effects of tryptophan depletion on neural responses to emotional words in remitted depression. Biol. Psychiatry. 2009; 66:441–450. [PubMed: 19539268]

Daly E, Deeley Q, Hallahan B, Craig M, Brammer M, Lamar M, Cleare A, Giampietro V, Ecker C, Page L, Toal F, Phillips ML, Surguladze S, Murphy DG. Effects of acute tryptophan depletion on neural processing of facial expressions of emotion in humans. Psychopharmacology. 2010; 210:499–510. [PubMed: 20424829]

Van der Veen FM, Evers EA, Mies GW, Vuurman EF, Jolles J. Acute tryptophan depletion selectively attenuates cardiac slowing in an Eriksen flanker task. J. Psychopharmacol. 2010; 24:1455–1463. [PubMed: 19304860]

Booij L, Van der Does AJ. Emotional processing as a predictor of symptom change: an acute tryptophan depletion study in depressed patients. Eur. Neuropsychopharmacol.: J. Eur Coll. Neuropsychopharmacol. 2011; 21:379–383.

Kunisato Y, Okamoto Y, Okada G, Aoyama S, Demoto Y, Munakata A, Nomura M, Onoda K, Yamawaki S. Modulation of default-mode network activity by acute tryptophan depletion is associated with mood change: a resting state functional magnetic resonance imaging study. Neurosci. Res. 2011; 69:129–134. [PubMed: 21078349]

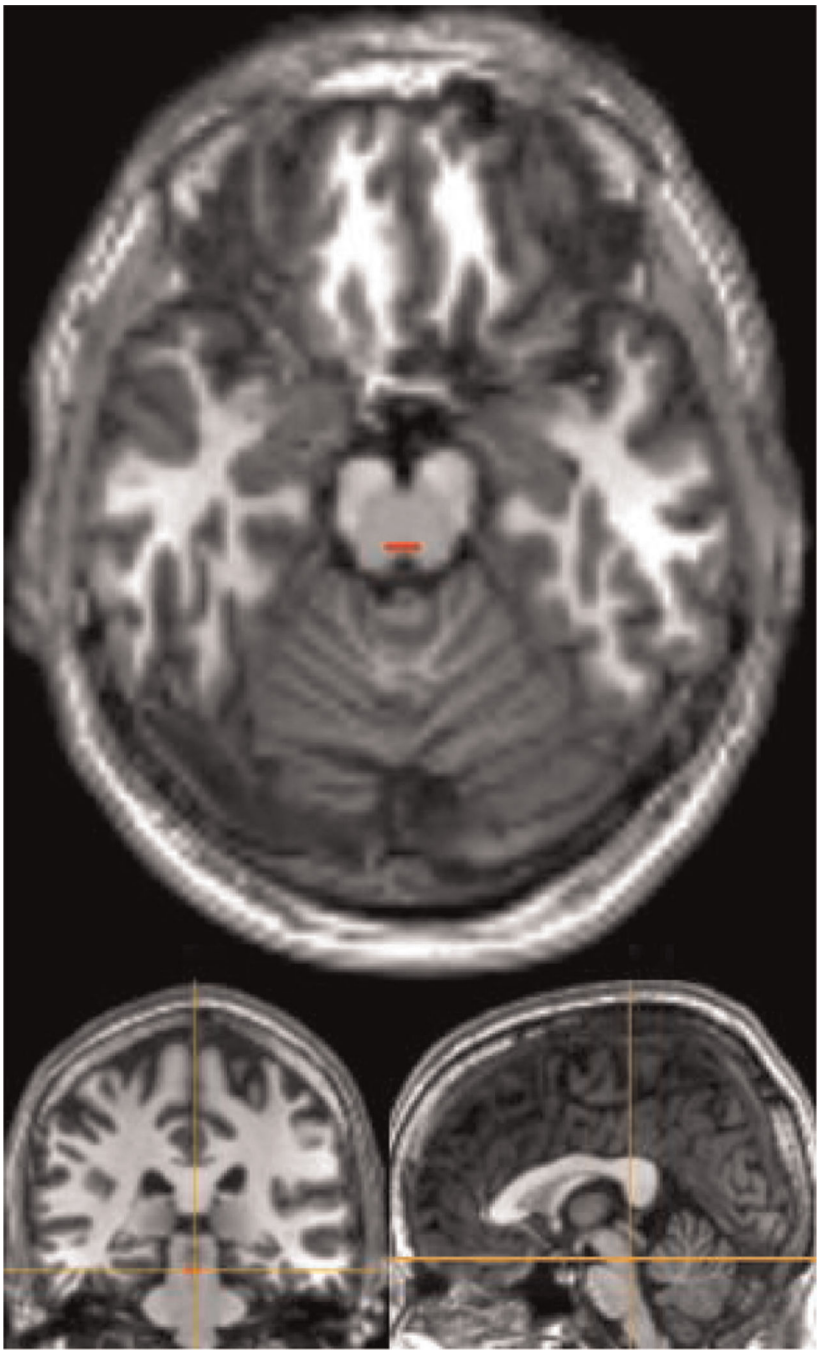

Fig. 1.
Example of a subject-specific dorsal raphé ROI after normalization.

Table 1

Regions of interest sizes, coordinates and literature-based selection criteria.

ROI	Chosen for	MNI coordinates
vmPFC	Anterior hub of DMN	0, 54, −8
dlPFC	Cognitive control network	−28, 22, 52 30, 22, 52
PCC	Posterior hub of DMN	0, −56, 28
pgACC	Altered functional connectivity in depression	−8, 41, 5 8, 41, 5
sgACC	Altered metabolism and functional connectivity in depression; Target for DBS treatments for depression	0, 21, −10
Anterior Thalamus	Rich serotonergic innervation with frontal projections	−10, −12, 12 10, −12, 12
Dorsal Raphé	Origin of serotonergic neurons; Involvement in action of SRI antidepressant treatments	Subject-specific

pgACC, sgACC, and anterior thalamus ROIs were conservatively created as 5 mm radius spheres. As standard in CONN toolbox, dlPFC, vmPFC, and PCC volumes approximated 10 mm radius spheres. For the dorsal raphé, each subject-specific rectangular volume was hand-drawn as detailed in the text. Raphé sizes ranged from 3 to 10 voxels of 8 mm^3.

DBS = deep brain stimulation; dlPFC = dorsolateral prefrontal cortex; DMN = default mode network; PCC = posterior cingulate cortex; pgACC = pregenual anterior cingulate cortex; ROI = region of interest; sgACC = subgenual anterior cingulate cortex; SRI = serotonin reuptake inhibitor; vmPFC = ventromedial prefrontal cortex.

Table 2

Changes in dorsal raphé resting-state functional connectivity with acute tryptophan depletion in SSRI-treated major depressive disorder.

Frequency band (Hz)	Participant group	Thalamus left		Thalamus right		pgACC left		pgACC right	
		ΔZ(*r*)	***p***	**ΔZ(*r*)**	***p***	**ΔZ(*r*)**	***p***	**ΔZ(*r*)**	***p***
0.01–0.1	All participants, *n* = 15	0.05	0.21	0.01	0.86	0.03	0.63	0.09	0.13
	Remitters, *n* = 10	0.08	0.16	0.00	0.95	−0.05	0.50	0.03	0.63
	Non-remitters, *n* = 5	−0.01	0.81	0.02	0.85	0.18	0.19	0.20	0.12
	Remitters vs. Non-rem.	0.10	0.28	−0.02	0.88	−0.22	0.09	−0.17	0.18
0.01–0.025	All participants	−0.17	0.15	−0.20	0.20	0.14	0.20	0.06	0.65
	Remitters	−0.14	0.28	−0.25	0.17	0.01	0.96	−0.01	0.96
	Non-remitters	−0.23	0.36	−0.10	0.76	0.41	0.10	0.21	0.29
	Remitters vs. Non-rem.	0.09	0.71	−0.15	0.64	−0.41	0.09	−0.22	0.47
0.025–0.05	All participants	**0.19**	**0.01**	**0.18**	**0.05**	−0.09	0.21	0.09	0.32
	Remitters	0.15	0.09	0.08	0.44	**−0.18**	**0.02**	0.08	0.46
	Non-remitters	**0.26**	**0.04**	0.38	0.07	0.09	0.58	0.10	0.51
	Remitters vs. Non-rem.	−0.11	0.39	−0.30	0.11	−0.27	0.08	−0.02	0.92
0.05–0.1	All participants	0.08	0.29	0.00	0.97	0.02	0.74	**0.12**	**0.03**
	Remitters	0.14	0.16	0.07	0.38	0.02	0.83	0.07	0.19
	Non-remitters	−0.06	0.52	−0.16	0.37	0.03	0.76	0.22	0.14
	Remitters vs. Non-rem.	0.20	0.19	0.23	0.16	−0.01	0.94	−0.15	0.18

Changes in functional connectivity (Δ*Z*(*r*)) between sham and ATD (*Z*(*r*) sham minus *Z*(*r*) ATD) for dorsal raphé to the selected ROIs. We also examined changes in functional connectivity of dorsal raphé with the bilateral dlPFC, and midline sgACC, vmPFC and PCC ROIs. These data are not presented in Table 2 because none of these regions demonstrated significantly altered functional connectivity with the dorsal raphé during ATD.

ATD = acute tryptophan depletion; dlPFC = dorsolateral prefrontal cortex; PCC = posterior cingulate cortex; pgACC = pregenual anterior cingulate cortex; sgACC = subgenual anterior cingulate cortex; SSRI = selective serotonin reuptake inhibitor; vmPFC = ventromedial prefrontal cortex.